

## *Supporting Information*

### **Addressing a Trapped High-Energy Water: Design and Synthesis of Highly Potent Pyrimidoindole-based GSK-3 $\beta$ inhibitors**

**Stanislav Andreev,<sup>1,‡</sup> Tatu Pantsar,<sup>1,2,‡</sup> Roberta Tesch,<sup>3,4</sup> Niclas Kahlke,<sup>1</sup> Ahmed El-Gokha,<sup>1,5</sup> Francesco Ansideri,<sup>1</sup> Lukas Grätz,<sup>6</sup> Jenny Romasco,<sup>7</sup> Giulia Sita,<sup>8</sup> Christian Geibel,<sup>9</sup> Michael Lämmerhofer,<sup>9</sup> Andrea Tarozzi,<sup>7</sup> Stefan Knapp,<sup>3,4</sup> Stefan A. Laufer<sup>1,10</sup> and Pierre Koch<sup>1,6,\*</sup>**

<sup>1</sup> Institute of Pharmaceutical Sciences, Department of Medicinal and Pharmaceutical Chemistry, Eberhard Karls University Tübingen, Auf der Morgenstelle 8, 72076 Tübingen, Germany

<sup>2</sup> School of Pharmacy, Faculty of Health Sciences, University of Eastern Finland, P.O. Box 1627, 70211 Kuopio, Finland

<sup>3</sup> Institute for Pharmaceutical Chemistry, Johann Wolfgang Goethe-University, Max-von-Laue-Str. 9, 60438 Frankfurt am Main, Germany

<sup>4</sup> Structural Genomics Consortium, Buchmann Institute for Life Sciences, Johann Wolfgang Goethe-University, Max-von-Laue-Str. 15, 60438 Frankfurt am Main, Germany

<sup>5</sup> Chemistry Department, Faculty of Science, Menoufia University, Gamal Abdel-Nasser Street, 32511 Shebin El-Kom, Egypt

<sup>6</sup> Department of Pharmaceutical/Medicinal Chemistry II, Institute of Pharmacy, University of Regensburg, Universitätsstraße 31, 93053 Regensburg, Germany

<sup>7</sup> Department for Life Quality Studies, Alma Mater Studiorum, University of Bologna, Corso D'Augusto 237, 47921 Rimini, Italy

<sup>8</sup> Department of Pharmacy and Biotechnology, Alma Mater Studiorum, University of Bologna, Via Irnerio 48, 40126 Bologna, Italy

<sup>9</sup> Institute of Pharmaceutical Sciences, Department of Pharmaceutical (Bio-)Analysis, Eberhard Karls University Tübingen, Auf der Morgenstelle 8, 72076 Tübingen, Germany

<sup>10</sup> Tübingen Center for Academic Drug Discovery (TüCAD2), Auf der Morgenstelle 8, 72076 Tübingen, Germany

‡ These authors contributed equally.

\* Correspondence: pierre.koch@uni-tuebingen.de, pierre.koch@ur.de; Tel.: +49 941 943-2847.

## Table of Contents

<b>ADP Glo<sup>TM</sup> Kinase Assay Protocol</b>	<b>S3</b>
<b>Figure S1.</b> Comparison of molecular surface areas among selected compounds ( <i>S</i> -isomers) based on Jaguar-optimized geometries.	<b>S4</b>
<b>Figure S2.</b> Comparison of the electrostatic potential and electron density of ( <i>S</i> )- <b>5c</b> , ( <i>S</i> )- <b>15</b> and ( <i>S</i> )- <b>5m</b> .	<b>S5</b>
<b>Figure S3.</b> WaterMap analysis of ( <i>S</i> )- <b>5m</b> and ( <i>S</i> )- <b>15</b> based on the ( <i>S</i> )- <b>5c</b> crystal structure.	<b>S6</b>
<b>Figure S4.</b> Molecular dynamics simulations of ( <i>S</i> )- <b>5c</b> and ( <i>S</i> )- <b>15</b> suggest no shift in interactions with GSK-3 $\beta$ among these compounds.	<b>S7</b>
<b>Figure S5.</b> The orientation and hydrogen bond interactions of the high-energy water molecule observed in the WaterMap simulations of ( <i>S</i> )- <b>5c</b> and ( <i>S</i> )- <b>15</b> .	<b>S8</b>
<b>NanoBRET target engagement assay</b>	<b>S9</b>
<b>Figure S6.</b> Cytotoxicity of <b>20</b> and ( <i>S</i> )- <b>15</b> in neuronal SH-SY5Y cells.	<b>S11</b>
<b>Figure S7.</b> Effects of <b>20</b> and ( <i>S</i> )- <b>15</b> on the GSK-3 activity in neuronal SH-SY5Y cells.	<b>S12</b>
<b>Figure S8.</b> Neuroprotective effects of <b>20</b> and ( <i>S</i> )- <b>15</b> against the neurotoxicity induced by H <sub>2</sub> O <sub>2</sub> in neuronal SH-SY5Y cells.	<b>S13</b>
<b>Materials and Methods for cellular assays in neuronal SH-SY5Y cells</b>	<b>S14</b>
<b>Kinome screening data for (<i>S</i>)-<b>15</b> and <b>22</b></b>	<b>S16</b>
<b>Figure S9.</b> Workflow of combining molecular dynamics simulations with WaterMap while evaluating new ligand designs.	<b>S18</b>
<b><sup>1</sup>H and <sup>13</sup>C NMR spectra of (<i>S</i>)-<b>5c</b>, (<i>S</i>)-<b>15</b>, <b>20</b> and <b>22</b></b>	<b>S19</b>
<b>HPLC chromatograms of (<i>S</i>)-<b>5c</b>, (<i>S</i>)-<b>15</b>, <b>20</b> and <b>22</b></b>	<b>S23</b>
<b>References</b>	<b>S27</b>

## **ADP Glo™ Kinase Assay Protocol**

The IC<sub>50</sub> values of the final compounds for GSK-3β were determined in an ADP Glo™ kinase assay from Promega (Madison, WI, USA).

The assay was carried out in white, non-treated 384-well plates from Corning (Corning, NY, USA). The experiments were carried out as duplicates or quadruplicates using a concentration of 0.58 ng/μL of recombinant human GSK-3β, 0.2 μg/μL GSK-3 substrate G50-58 (sequence: YRRAAVPPSPSLSRHSSPHQ(pS)EDEEE) and 25 μM ATP in the presence of serial dilutions of the final compounds (six 1:3 or 1:4 dilution steps starting from 10 μM). Two control experiments with uninhibited kinase and blank experiments with ATP/substrate solution were performed and their results were used for the normalization of the raw data.

In detail, GSK-3β was pre-incubated with the final compounds for 10 min at rt. Then substrate/ATP was added to start the reaction, which was run for 1 h at rt. ADP Glo™ reagent (5 μL, then 1 h incubation) and Kinase detection reagent (10 μL, then 30 min incubation) were subsequently added. The luminescence was finally measured on a FilterMax F5 microplate reader from Molecular Devices LLC (San José, CA, USA) (integration time 500 ms). The raw data was normalized and absolute IC<sub>50</sub> values were generated with PRISM v.7.03. from GraphPad Software (San Diego, CA, USA).

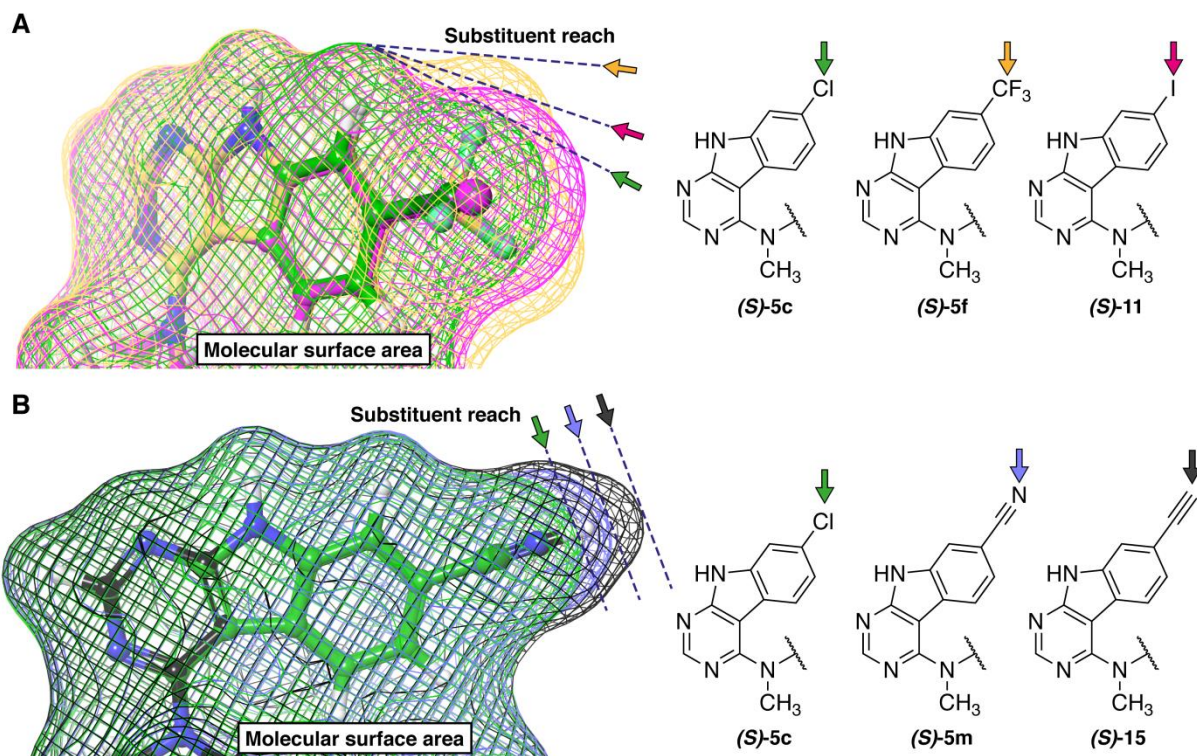
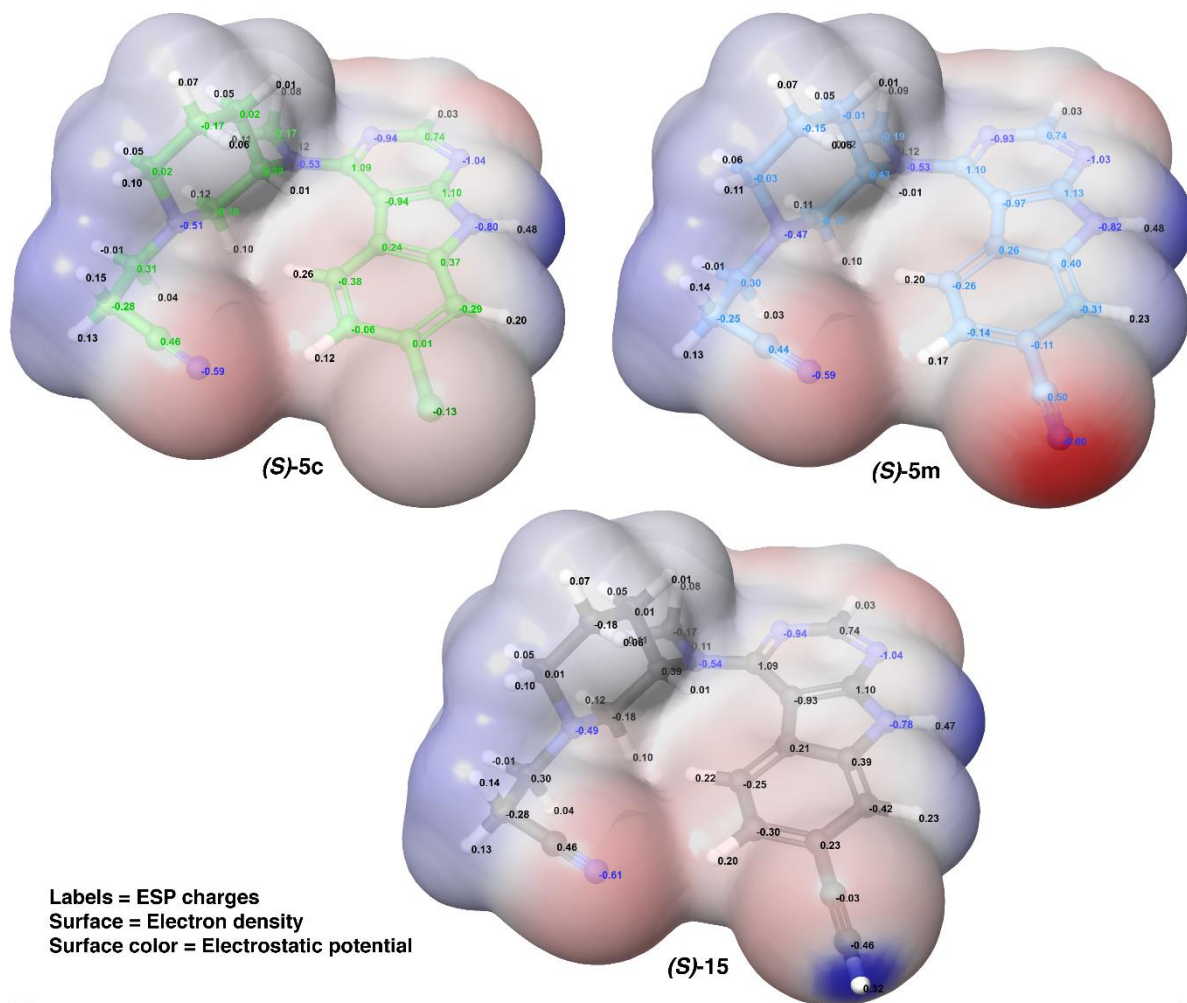


**Figure S1.** Comparison of molecular surface areas among selected compounds (*S*-isomers) based on Jaguar-optimized geometries. **(A)** Compared to (*S*)-5c, the substituents of (*S*)-5f and (*S*)-11 have considerably larger radii, which will most likely result in a clash with the gatekeeper residue Leu132. **(B)** Compared to (*S*)-5c, the substituents of (*S*)-5m and (*S*)-15 reach deeper towards the HR-I but do not significantly increase the molecular radius (compare to (*S*)-5f and (*S*)-11 in A). Molecular surfaces were generated by Maestro (Schrödinger LLC).



-0.3

Electrostatic Potential

0.3

**Figure S2.** Comparison of the electrostatic potential and electron density of *(S)*-**5c**, *(S)*-**5m** and *(S)*-**15**. Atomic electrostatic potential (ESP) charges were calculated with Jaguar (6-31G\*\*+, PBF water solvent model).

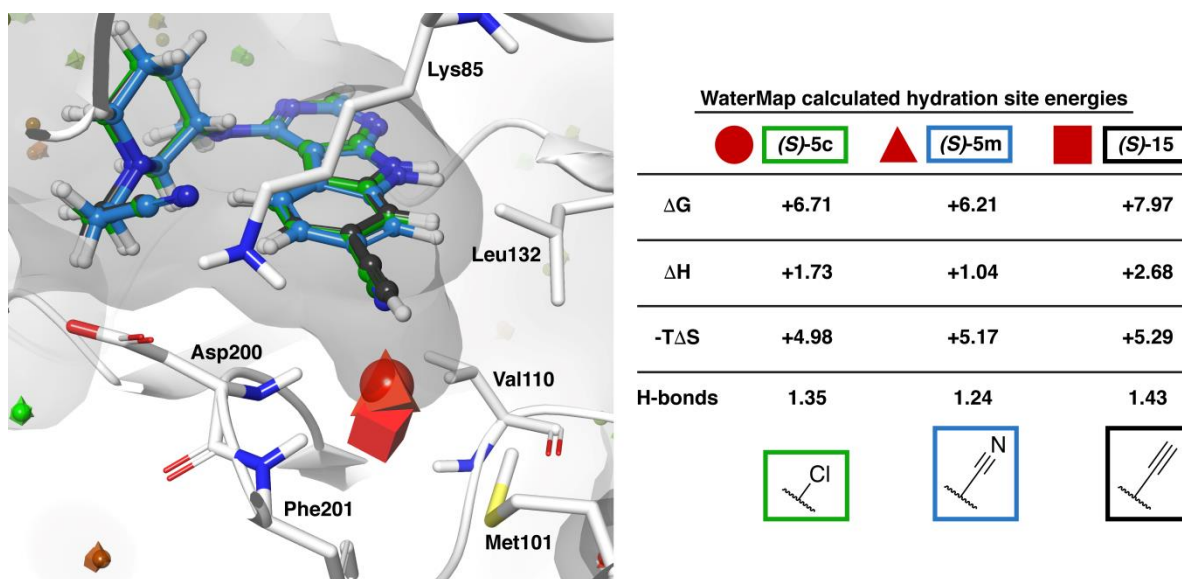


**Figure S3.** WaterMap analysis of (*S*)-**5m** and (*S*)-**15** based on the (*S*)-**5c** crystal structure. No shift of the high-energy hydration site is observed with (*S*)-**5m** (pyramid) compared to (*S*)-**5c** (sphere), whereas (*S*)-**15** clearly shifts the hydration site position (cube). A slightly lower free energy value is observed with (*S*)-**5m** compared to (*S*)-**5c**. The shifted hydration site of (*S*)-**15** displays an extremely high free energy value.

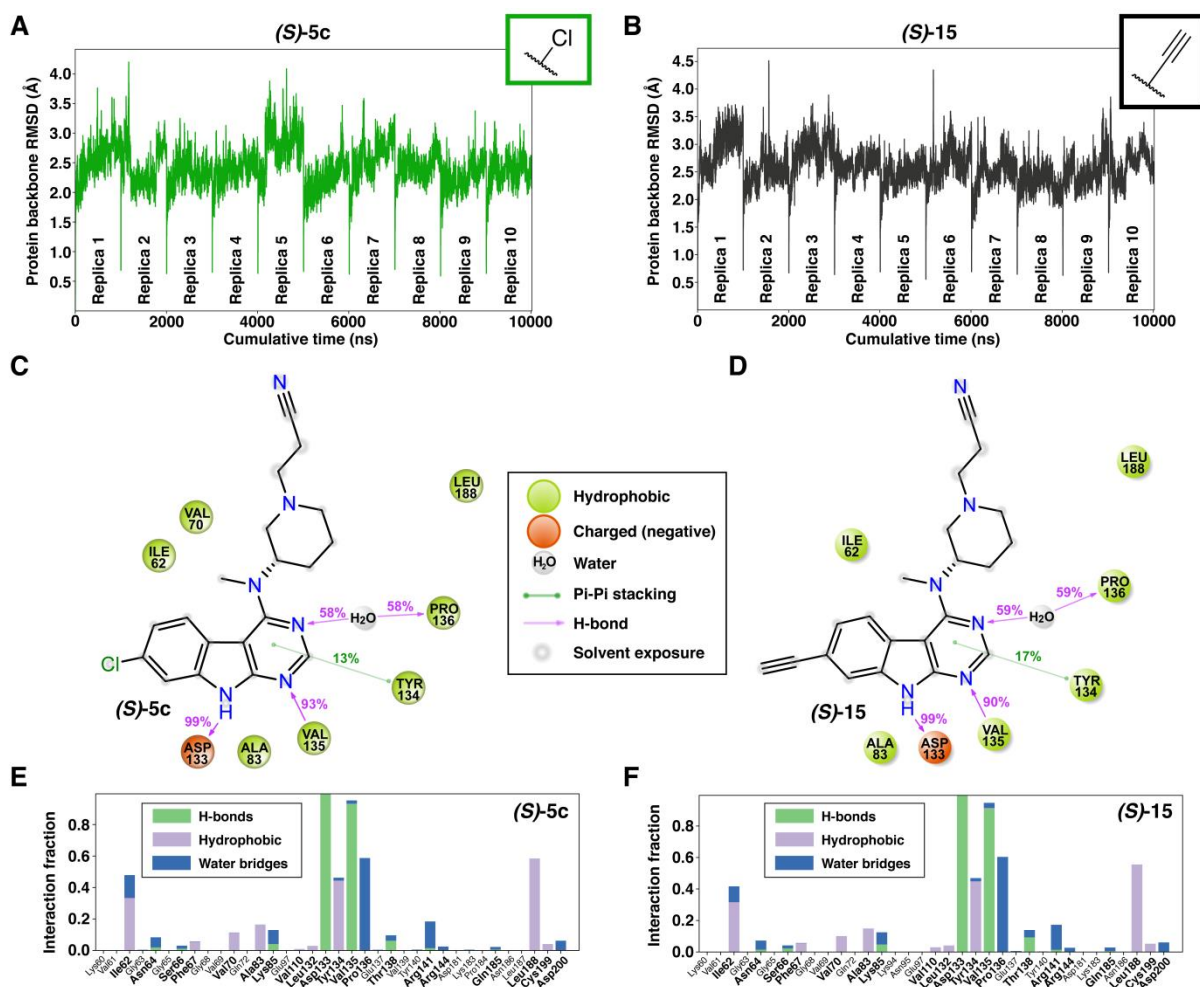


**Figure S4.** Molecular dynamics simulations of *(S)*-5c and *(S)*-15 suggest no shift in interactions with GSK-3β among these compounds. Root-mean-square deviation (RMSD) values of protein backbone atoms in ten 1 μs replica simulations of *(S)*-5c (**A**) and *(S)*-15 (**B**). Nearly identical interactions and their frequencies are observed with both compounds throughout the simulations. The observed main ligand–protein contacts are shown in the 2D-representations (**C**, **D**) and all contacts in the histogram-plots (**E**, **F**).



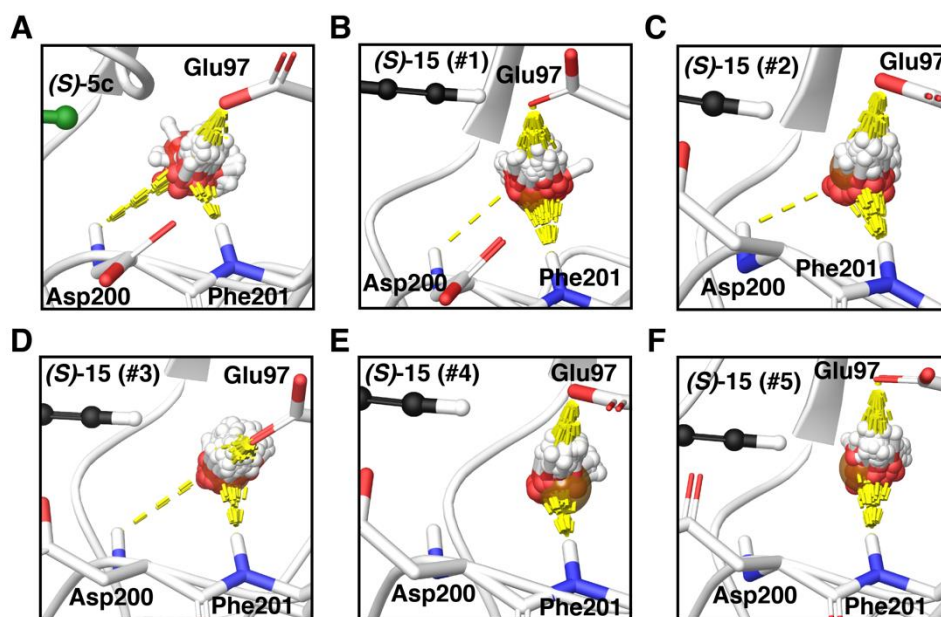


**Figure S5.** The orientation and hydrogen bond interactions of the high-energy water molecule observed in the WaterMap simulations of (*S*)-**5c** and (*S*)-**15**. In the case of (*S*)-**15**, the slight shift in the position of the water molecule results in the loss of the hydrogen bond to Asp200 along with improved hydrogen bonding with Phe201 and Glu97 (**B–F**). This shift in the position and altered hydrogen bonding correlate with the enthalpic gain (decrease in energy): the biggest benefit in gain in enthalpy is observed with (**E**) #4 (-1.93 kcal/mol) and (**F**) #5 (-1.48 kcal/mol), where all water molecule conformations display interactions solely to Phe201 and Glu97. Lowest gain in enthalpy is observed with (**D**) #3 (0.06 kcal/mol), where in two conformations the hydrogen bond to Asp200 still exists.



### **NanoBRET target engagement assay**

HEK293T cells (kind gift from Prof. Dr. Wulf Schneider, Institute for Medical Microbiology and Hygiene, University Hospital Regensburg, Germany) were routinely maintained in DMEM (Dulbecco's Modified Eagle's Medium, Sigma-Aldrich, Munich, Germany), supplemented with 10% FCS (Sigma-Aldrich, Munich, Germany), at 37 °C in a water-saturated atmosphere (5% CO<sub>2</sub>). All cells were routinely checked for mycoplasma infection using the Venor GeM Mycoplasma Detection Kit (Minerva Biolabs, Berlin, Germany).

HEK293T cells stably expressing NLuc-GSK3 $\beta$  were generated according to a described procedure with the exception that the amount of transfected cDNA was reduced to 1  $\mu$ g.<sup>1</sup> The cDNA encoding NLuc-GSK3 $\beta$  was kindly provided by Promega (Mannheim, Germany). Stably transfected cells were selected in the presence of 1 mg/mL G418 (Fisher Scientific, Nidderau, Germany). For further cultivation of the stable transfectants, the concentration of G418 was reduced to 600  $\mu$ g/mL.

After reaching  $\approx$  80-90% confluency, the stably transfected cells were detached with trypsin/EDTA (0.05%/0.02%, Biochrom, Berlin, Germany) and centrifuged (500 g, 5 min). The cell pellet was resuspended in Leibovitz' L-15 medium (L-15, Fisher Scientific, Nidderau, Germany), supplemented with 5% FCS and 10 mM HEPES (Sigma-Aldrich, Munich, Germany). After adjusting the cell density to 6.25 x 10<sup>5</sup> cells/mL, 80  $\mu$ L of the cell suspension were added to each well of a white 96-well plate (Brand, Wertheim, Germany) and incubated overnight at 37 °C (no additional CO<sub>2</sub>).

On the day of the experiment, serial dilutions of the test compounds (10-fold more concentrated than the final assay concentration) were prepared in L-15 + 10 mM HEPES. The fluorescent tracer K-8 (Promega, Mannheim, Germany) was diluted in DMSO to a concentration of 4  $\mu$ M (100-fold more concentrated than the final assay concentration). This was further diluted 10-fold using the Tracer Dilution Buffer (Promega, Mannheim, Germany) yielding a dilution, which was 10-fold concentrated to the final assay concentration. Next, 10  $\mu$ L of the final fluorescent tracer dilution were added to the cells (final concentration of K-8 in the assay: 0.04  $\mu$ M) and the plate was shaken for 10 seconds (orbital, 250 rpm). After adding 10  $\mu$ L of the serial dilutions of the respective test compounds, the plate was shaken again for 10 seconds (orbital, 250 rpm). A solvent control (0%) and a positive control, which contained solely the fluorescent tracer K-8 but no test compound, were included in each experiment. After incubating the plate at 37 °C for 2 h, the plate was equilibrated to room temperature for 15 min.

Next, 10  $\mu\text{L}$  of the detection reagent (consisting of 1192  $\mu\text{L}$  L-15 + 6  $\mu\text{L}$  NanoBRET NanoGlo Substrate + 2  $\mu\text{L}$  Extracellular NanoLuc Inhibitor; substrate and inhibitor were purchased from Promega, Mannheim, Germany) were added to each well on the plate and the measurement was started. All measurements were performed at room temperature using a TECAN InfiniteLumi plate reader (TECAN Austria GmbH, Grödig, Austria). The bioluminescence of NLuc was detected using a 460/35 nm band-pass filter. The fluorescence of the fluorescent tracer K-8 was detected using a 610 nm long-pass filter. Integration times were set to 1000 ms for both channels. The raw BRET ratio was calculated by dividing the emission of the fluorescent acceptor (measured with the 610 nm long-pass filter) by the donor luminescence (measured with the 460/35 nm band-pass filter). The obtained data were analyzed by a four-parameter logistic equation (GraphPad Prism 8.0, GraphPad Software Inc., San Diego, CA, USA) yielding  $\text{IC}_{50}$  values, for which means and the SEM were calculated.

**Table S1.** Cellular target engagement of compounds *(S)*-**5c**, *(S)*-**15**, **20** and **22** determined by a nanoBRET assay (n = 3).

<b>Compound</b>	<i>(S)</i> - <b>5c</b>	<i>(S)</i> - <b>15</b>	<b>20</b>	<b>22</b>
<b><math>\text{IC}_{50} \pm \text{SEM}</math> [<math>\mu\text{M}</math>]</b>	10.31 $\pm$ 1.53	2.51 $\pm$ 0.16	5.27 $\pm$ 0.24	2.40 $\pm$ 0.017

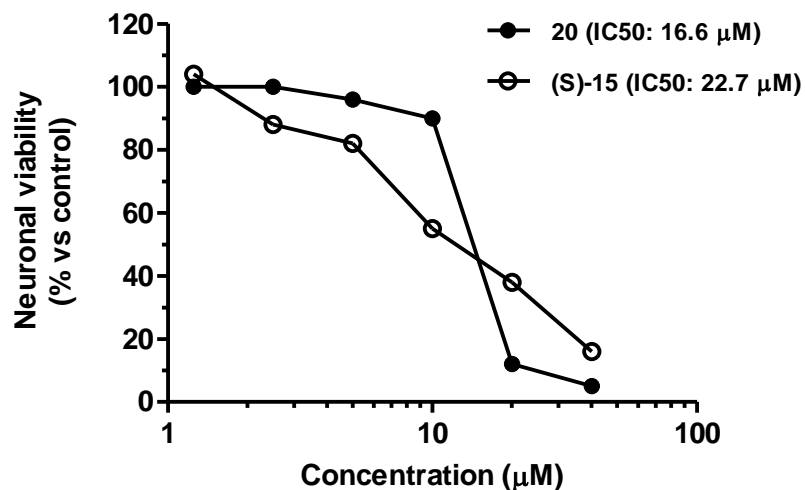


**Figure S6.** Cytotoxicity of **20** and (*S*)-**15** in SH-SY5Y cells. Cells were incubated for 24 h with different concentrations of the studied compounds [1.25 - 40 µM]. At the end of incubation, the neuronal viability was measured using MTT assay. Data are expressed as percentage of neuronal viability versus untreated cells and reported as mean of two independent experiments. IC<sub>50</sub> value: concentration resulting in 50% inhibition of neuronal viability.

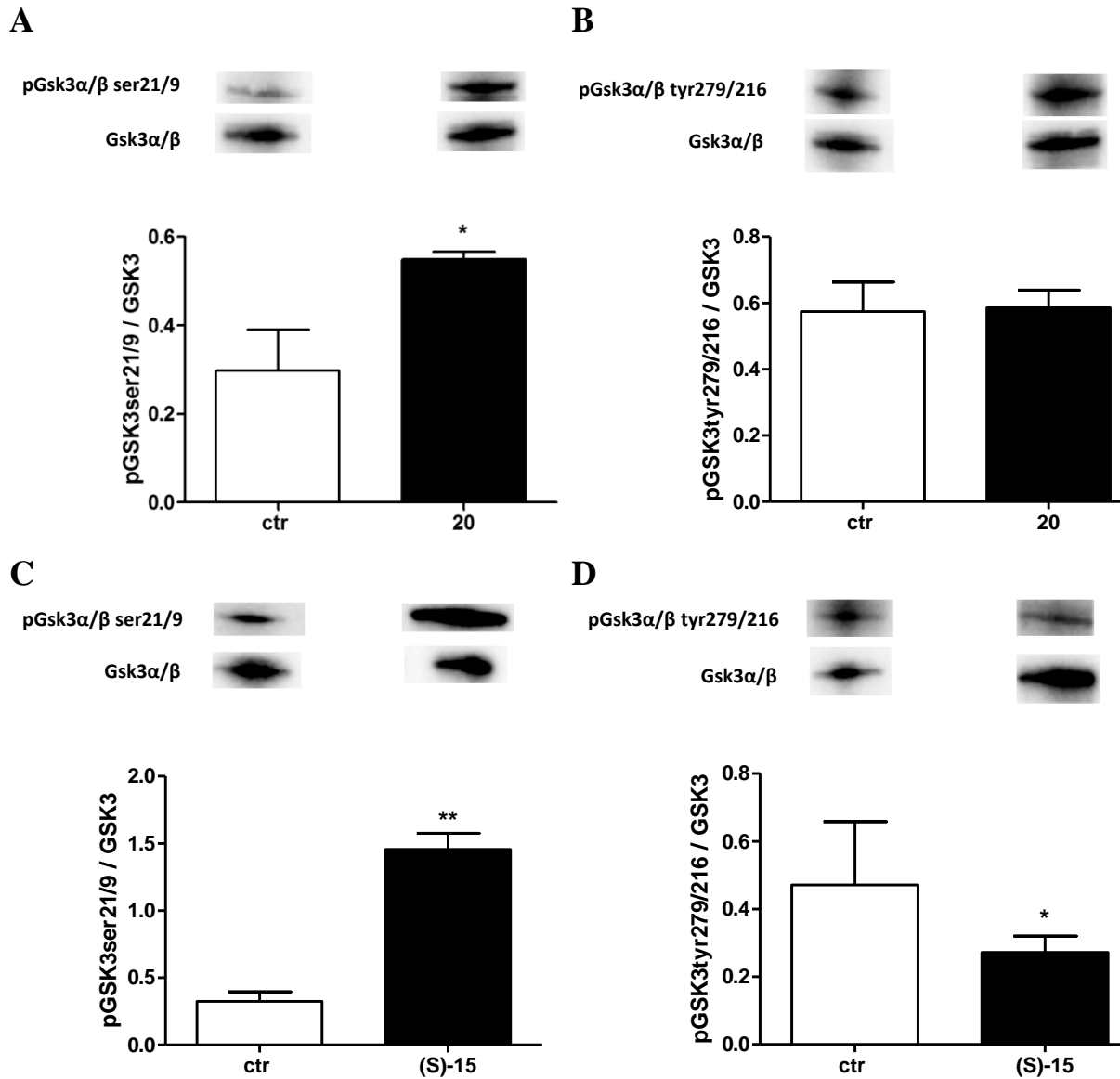


**Figure S7.** Effects of **20** and **(S)-15** on the GSK-3 activity in neuronal SH-SY5Y cells. Cells were incubated with **20** and **(S)-15** (5  $\mu$ M) for 3 h. At the end of incubation, the phosphorylation of GSK3 $\alpha/\beta$  on Ser21/9 (inactive GSK3 $\alpha/\beta$  form) (**A** for **20**, **C** for **(S)-15**) and on Tyr279/Tyr216 (active GSK3 $\alpha/\beta$  form) (**B** for **20**, **D** for **(S)-15**), respectively, was determined by western blotting. Data are expressed as ratio between phospho-GSK3 $\alpha/\beta$  and total GSK-3 levels normalized against  $\beta$ -Actin and reported as mean  $\pm$  SD of at least three independent experiments (\* $p < 0.05$  and \*\* $p < 0.01$  vs untreated cells).

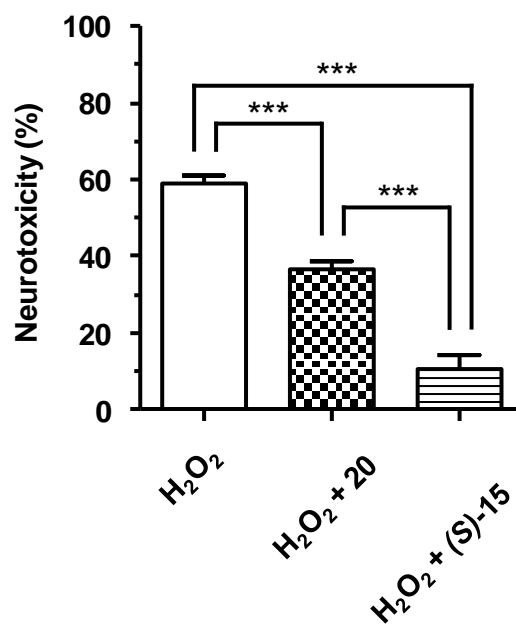


**Figure S8.** Neuroprotective effects of **20** and (*S*)-**15** against the neurotoxicity induced by H<sub>2</sub>O<sub>2</sub> in neuronal SH-SY5Y cells. Cells were incubated with **20** and (*S*)-**15** (5 μM) and H<sub>2</sub>O<sub>2</sub> (100 μM) for 1 h and then starved in complete medium for 22 h. The neurotoxicity was then evaluated by MTT assay as reported in materials and methods section. Data are expressed as percentages of neurotoxicity versus untreated cells and reported as mean ± SD of three independent experiments (\*\*\*p < 0.001).

## **Materials and methods for cellular assays in neuronal SH-SY5Y cells**

### **Cell cultures**

Human neuronal SH-SY5Y cells (Sigma Aldrich, St. Louis, MO, USA) were routinely grown in Dulbecco's modified Eagle's Medium supplemented with 10 % fetal bovine serum, 2 mM L-glutamine, 50 U/mL penicillin and 50 µg/mL streptomycin at 37 °C in a humidified incubator with 5 % CO<sub>2</sub>.

### **Neuronal viability**

SH-SY5Y cells were seeded in a 96-well plate at  $2 \times 10^4$  cells/well, incubated for 24 h and then treated with various concentrations (1.25-40 µM) of **20** and (*S*)-**15** for 24 h. Cell viability, in terms of mitochondrial activity, was evaluated by MTT assay, as previously described.<sup>2</sup>

### **Neuroprotective activity toward H<sub>2</sub>O<sub>2</sub>**

SH-SY5Y cells were seeded in a 96-well plate at  $2 \times 10^4$  cells/well, incubated for 24 h and subsequently treated with **20** and (*S*)-**15** (5 µM) and H<sub>2</sub>O<sub>2</sub> (100 µM) for 1 h. Then, cells were starved in complete medium for 22 h. The neuroprotective activity was measured by using the MTT assay as previously described.<sup>3</sup> Data are expressed as a percentage of neurotoxicity versus untreated cells.

### **Western blotting**

SH-SY5Y cells were seeded in 60 mm dishes at  $2 \times 10^6$  cells/dish, incubated for 24 h and subsequently treated with **20** and (*S*)-**15** (5 µM) for 3 h at 37°C in 5% CO<sub>2</sub>. At the end of incubation, cells were trypsinized and the cellular pellet was resuspended in complete lysis buffer containing leupeptin (2µg/mL), PMSF (100µg/mL) and cocktail of protease/phosphatase inhibitors (100×). Small amounts were removed for the determination of the protein concentration using the Bradford method. The samples (30 µg proteins) were run on 4-15% SDS polyacrylamide gels (Bio-rad Laboratories S.r.L., Hercules, CA, USA) and electroblotted onto 0.45 µm nitrocellulose membranes. The membranes were incubated at 4 °C overnight with primary antibody recognizing phospho-GSK3α/β (Ser21/9), (1:1000; Cell Signaling Technology Inc, Danvers, MA, USA), or anti-phospho-GSK3(Tyr279/Tyr216), (1:1000; EMD Millipore, Darmstadt, Germany). After washing with TBS-T (TBS +0.05% Tween20), the membranes were incubated with secondary antibodies (1:2000; GE Healthcare). Enhanced chemiluminescence was used to visualize the bands (ECL; Bio-rad Laboratories). The

membranes were then reprobod with GSK3 $\alpha/\beta$ , (1:1000; Cell Signaling Technology Inc.). The data were analyzed by densitometry, using Quantity One software (Bio-Rad Laboratories® S.r.L.). The values were normalized and expressed as mean  $\pm$  SD of densitometry in each experimental group.

**Statistical Analysis.** Results are shown as mean  $\pm$  standard deviation (SD) of three independent experiments. Statistical analysis was performed using Student's t-test and One-way ANOVA (post-hoc Bonferroni test). Differences were considered significant at  $p < 0.05$ . Analyses were performed using GraphPad PRISM software (version 5.0; GraphPad Software, La Jolla, CA, USA) on a Windows platform.



## Kinome screening data for inhibitors (S)-15 and 22

The selectivity of inhibitors (S)-15 and 22 was evaluated by the Eurofins KinaseProfiler™ (Eurofins Cerep, Celle l'Evescault, France) on 57 human kinases. The percentage residual activity of each kinase at an inhibitor concentration of 500 nM was determined and is reported in Table S2.

**Table S2.** Selectivity data of (S)-15 and 22 on 57 human kinases. Residual kinase activity is reported in percentage. Values below 50% are highlighted in red.

	(S)-15	22
Abl(h)	79	82
ALK(h)	71	90
AMPK $\alpha$ 1(h)	103	95
ASK1(h)	94	122
Aurora-A(h)	80	97
CaMKI(h)	86	94
CDK1/cyclinB(h)	113	85
CDK2/cyclinA(h)	77	79
CDK6/cyclinD3(h)	100	85
CDK7/cyclinH/MAT1(h)	86	80
CDK9/cyclin T1(h)	75	76
CHK1(h)	86	99
CK1 $\gamma$ 1(h)	123	115
CK2 $\alpha$ 2(h)	97	105
c-RAF(h)	80	98
DRAK1(h)	85	100
eEF-2K(h)	90	77
EGFR(h)	94	101
EphA5(h)	90	57
EphB4(h)	94	97
Fyn(h)	16	6
GSK3 $\beta$ (h)	3	-5
IGF-1R(h)	99	104
IKK $\alpha$ (h)	103	111
IRAK4(h)	97	118
JAK2(h)	129	79
KDR(h)	22	8
LOK(h)	19	11
Lyn(h)	31	25
MAPKAP-K2(h)	71	111
MEK1(h)	85	77
MLK1(h)	61	39
Mnk2(h)	82	92
MSK2(h)	84	33
MST1(h)	72	67

**Table S2.** continued.

	(S)-15	22
mTOR(h)	93	103
NEK2(h)	94	92
p70S6K(h)	99	79
PAK2(h)	77	83
PDGFR $\beta$ (h)	67	72
<b>Pim-1(h)</b>	<b>36</b>	<b>28</b>
PKA(h)	87	89
PKB $\alpha$ (h)	91	94
PKC $\alpha$ (h)	99	87
PKC $\theta$ (h)	82	75
PKG1 $\alpha$ (h)	84	75
Plk3(h)	109	113
PRAK(h)	91	99
ROCK-I(h)	84	90
Rse(h)	99	78
<b>Rsk1(h)</b>	<b>28</b>	<b>12</b>
SAPK2a(h)	107	126
SRPK1(h)	109	121
TAK1(h)	53	88
PI3 Kinase (p110 $\beta$ /p85 $\alpha$ )(h)	98	100
PI3 Kinase (p120 $\gamma$ )(h)	95	99
PI3 Kinase (p110 $\delta$ /p85 $\alpha$ )(h)	68	97
PI3 Kinase (p110 $\alpha$ /p85 $\alpha$ )(h)	96	100

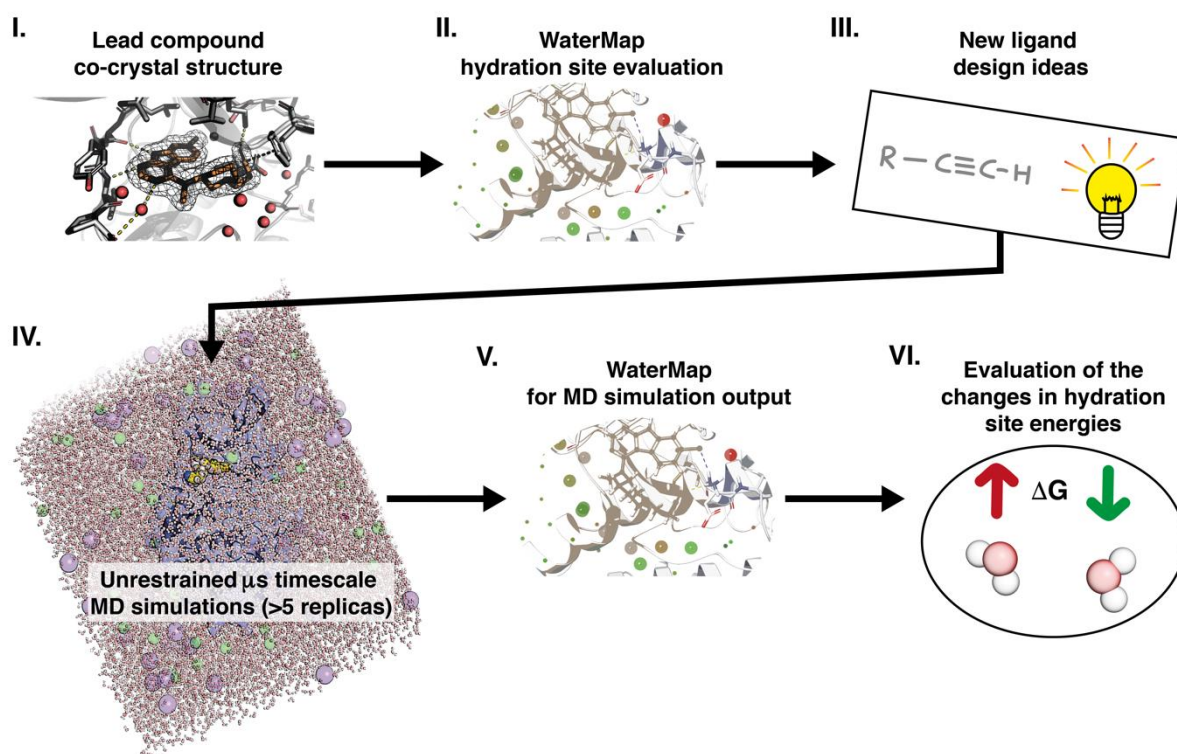
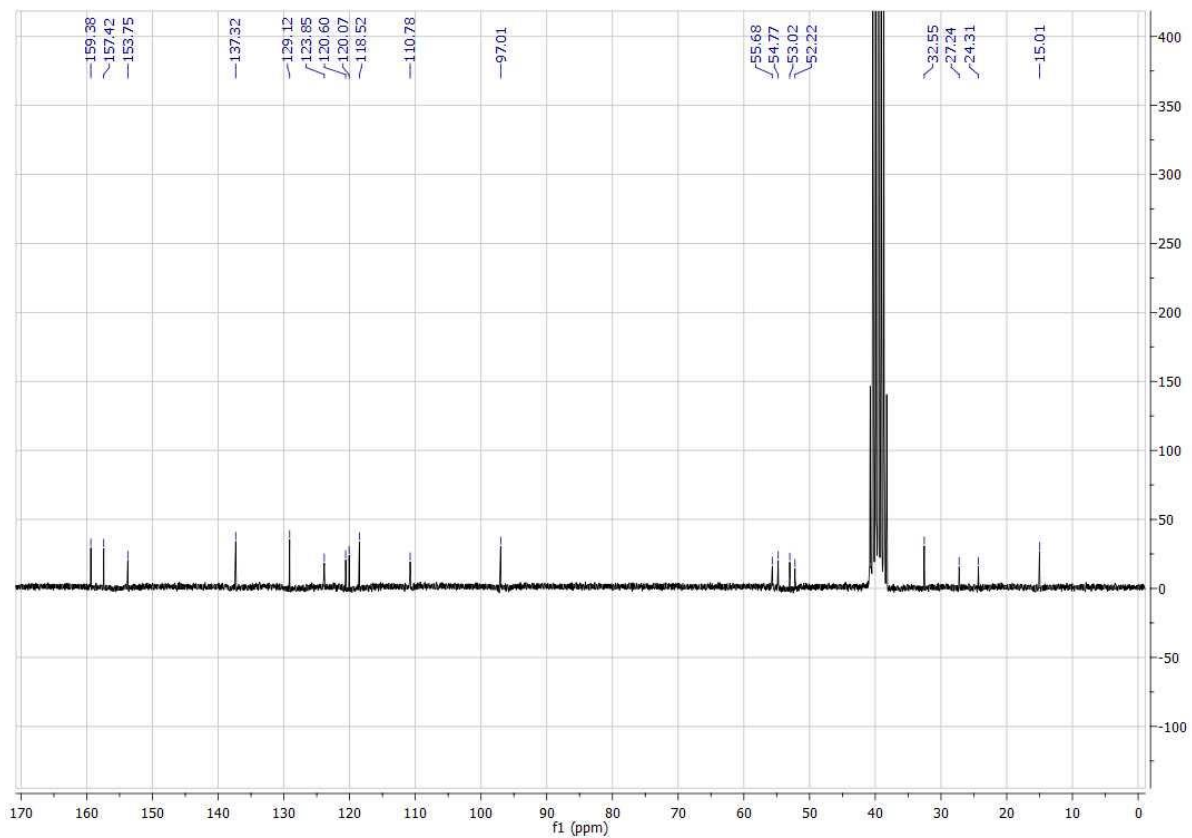
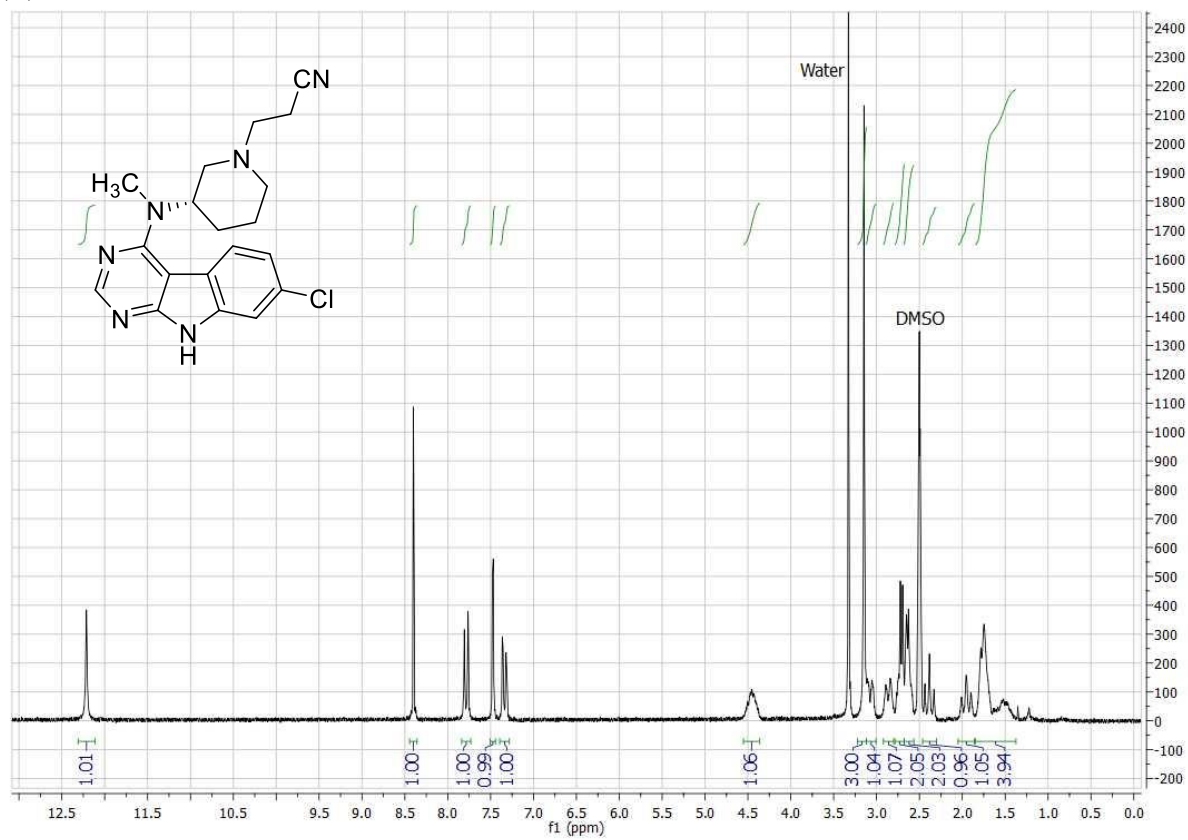


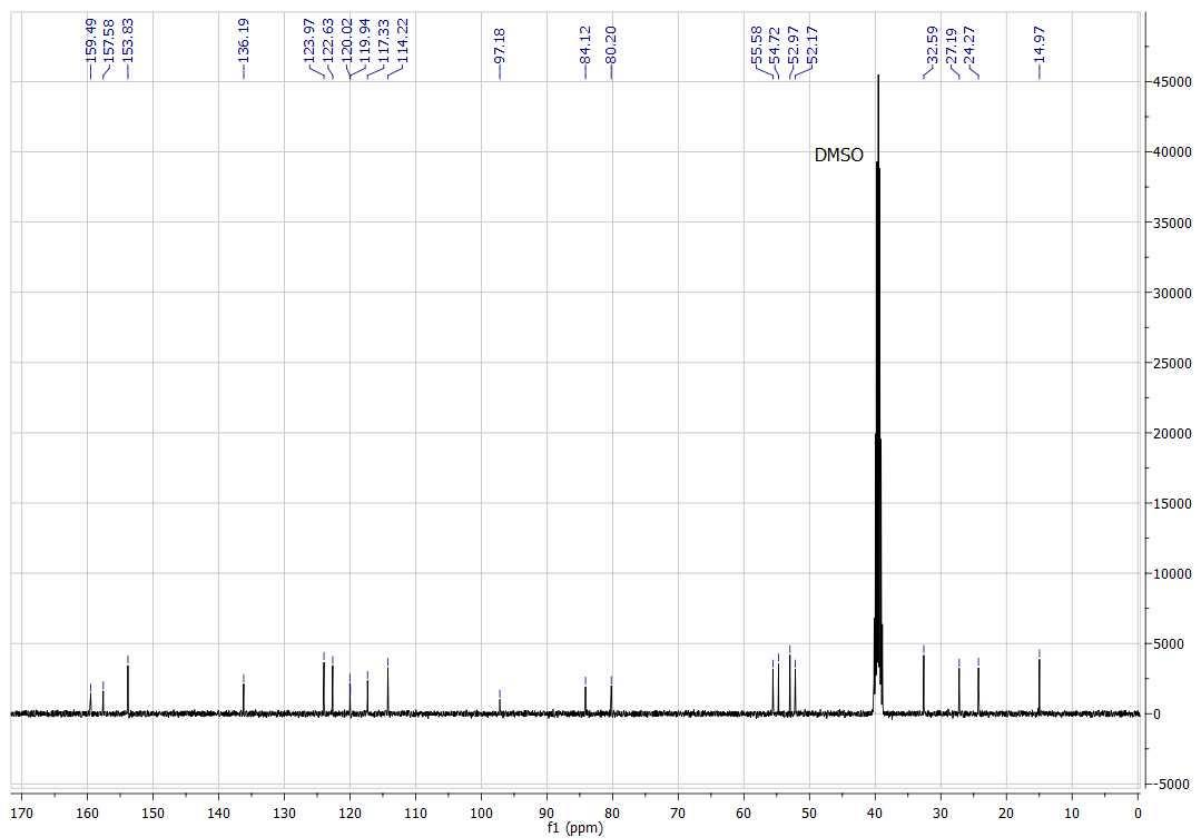
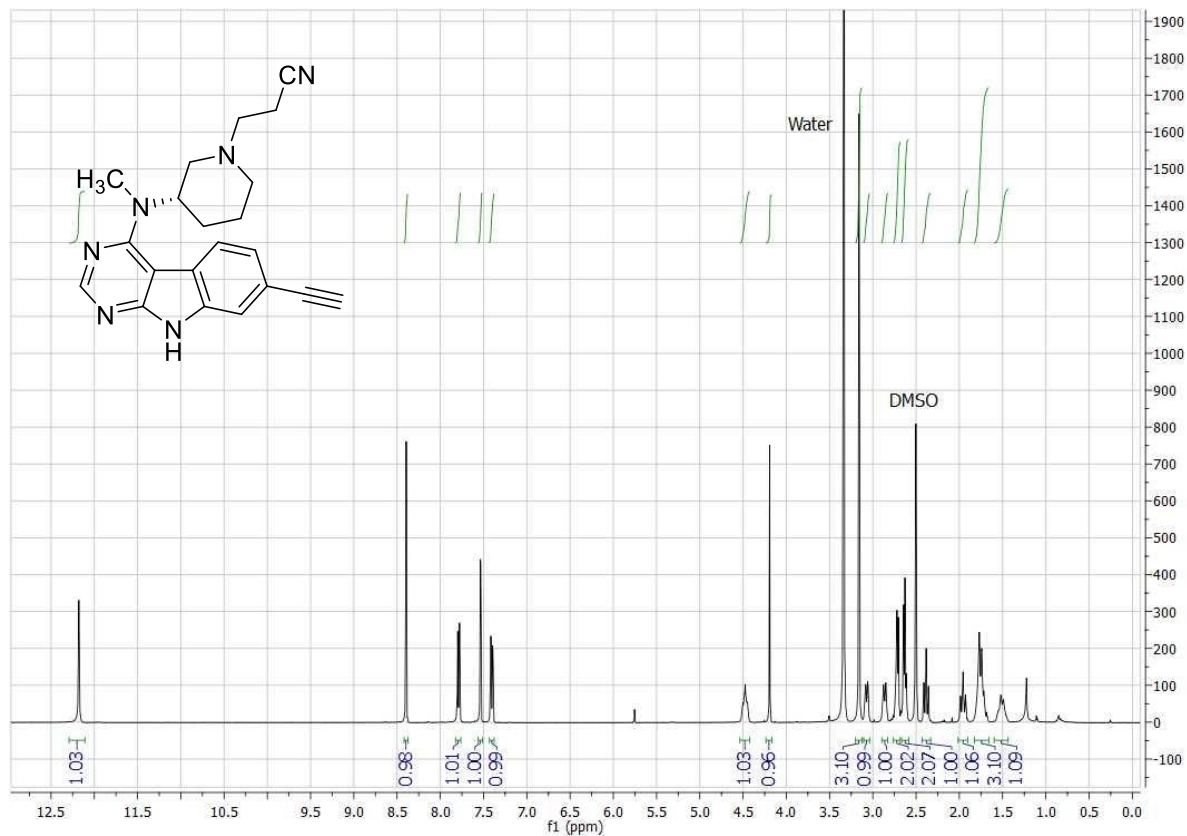
**Figure S9.** Workflow of combining molecular dynamics simulations with WaterMap while evaluating new ligand designs. **(I.)** Obtain/use crystal structure with reasonable resolution with the lead structure. **(II.)** Evaluate the hydration site energies to find out potential hydration sites to target. **(III.)** Design new ligands based on the potential high-energy hydration sites. **(IV.)** Run classical MD simulations to relax the new protein-ligand system. Note that it is obligatory to include several replicas to limit the random bias in the results. **(V.)** Run WaterMap for the MD simulation output structures (include several replicas). **(VI.)** Based on the WaterMap results, evaluate if the new design is beneficial or not in the context of shifted hydration site energies.

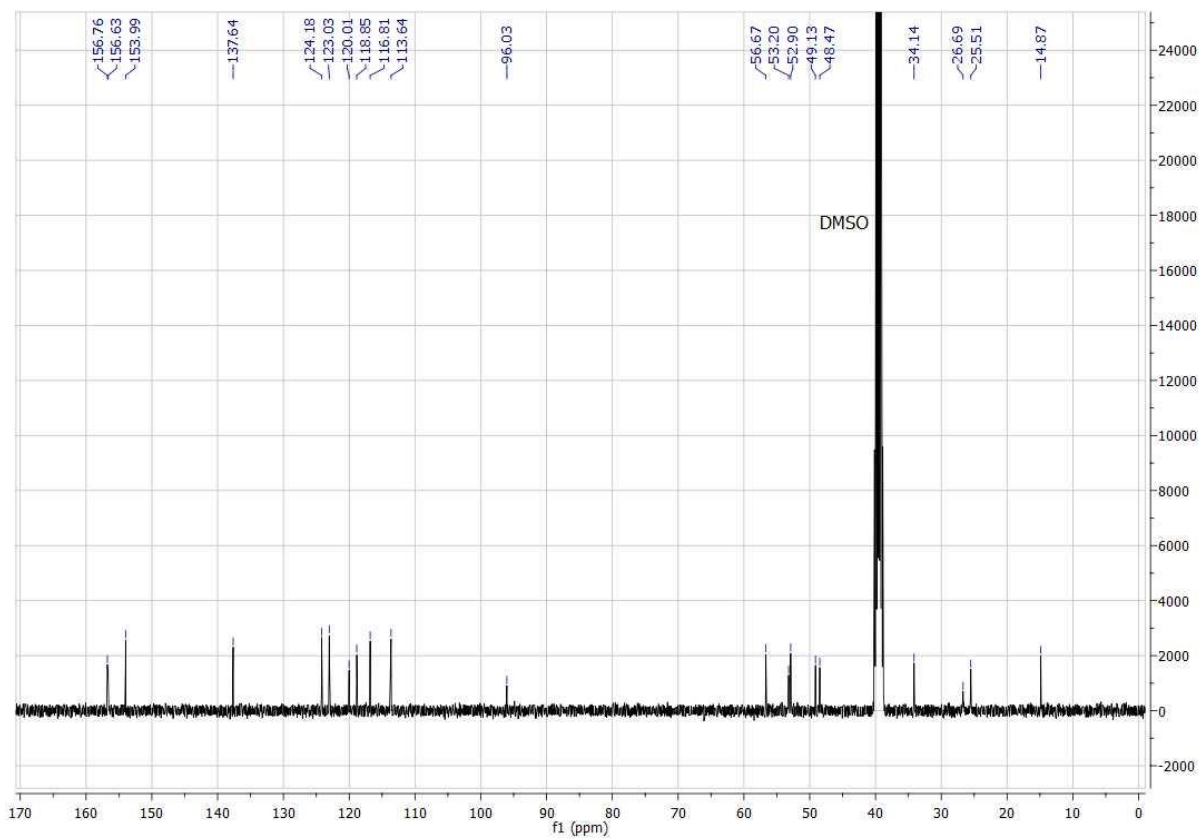
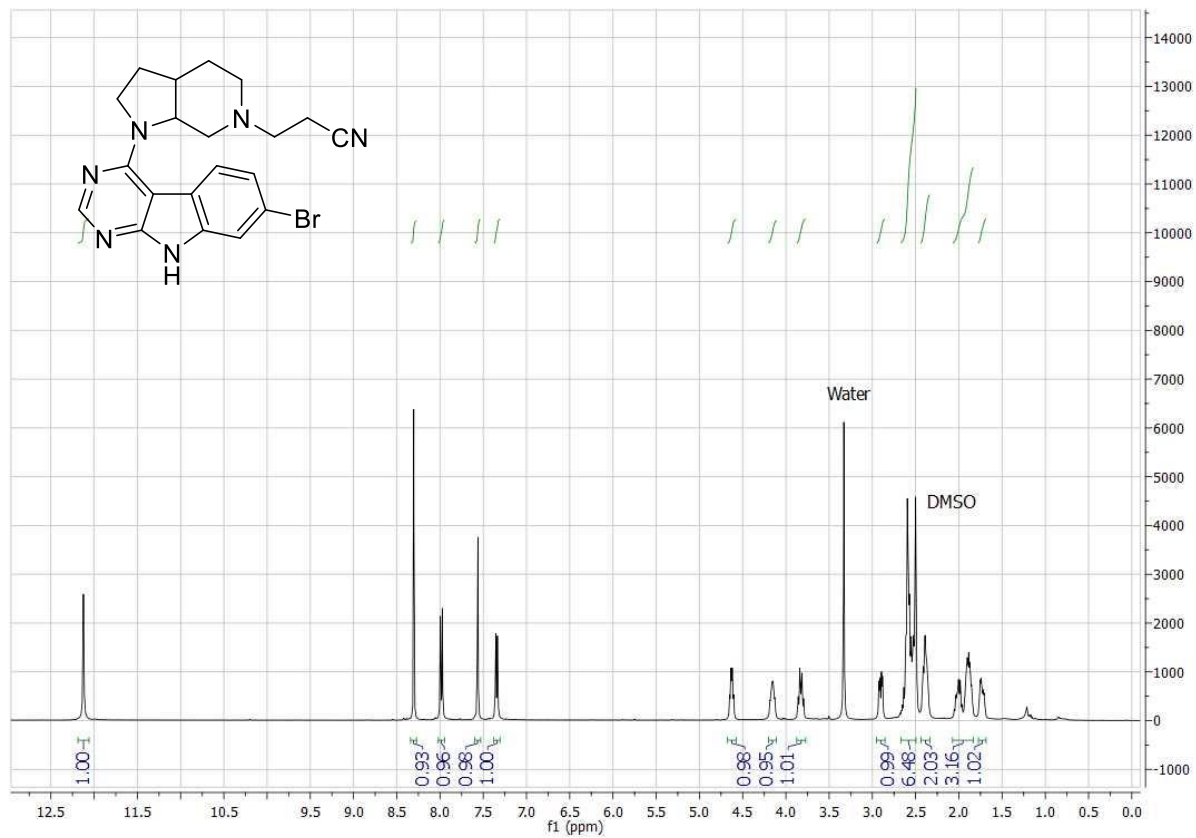
# $^1\text{H}$ and $^{13}\text{C}$ NMR spectra of (S)-5c, (S)-15, 20 and 22

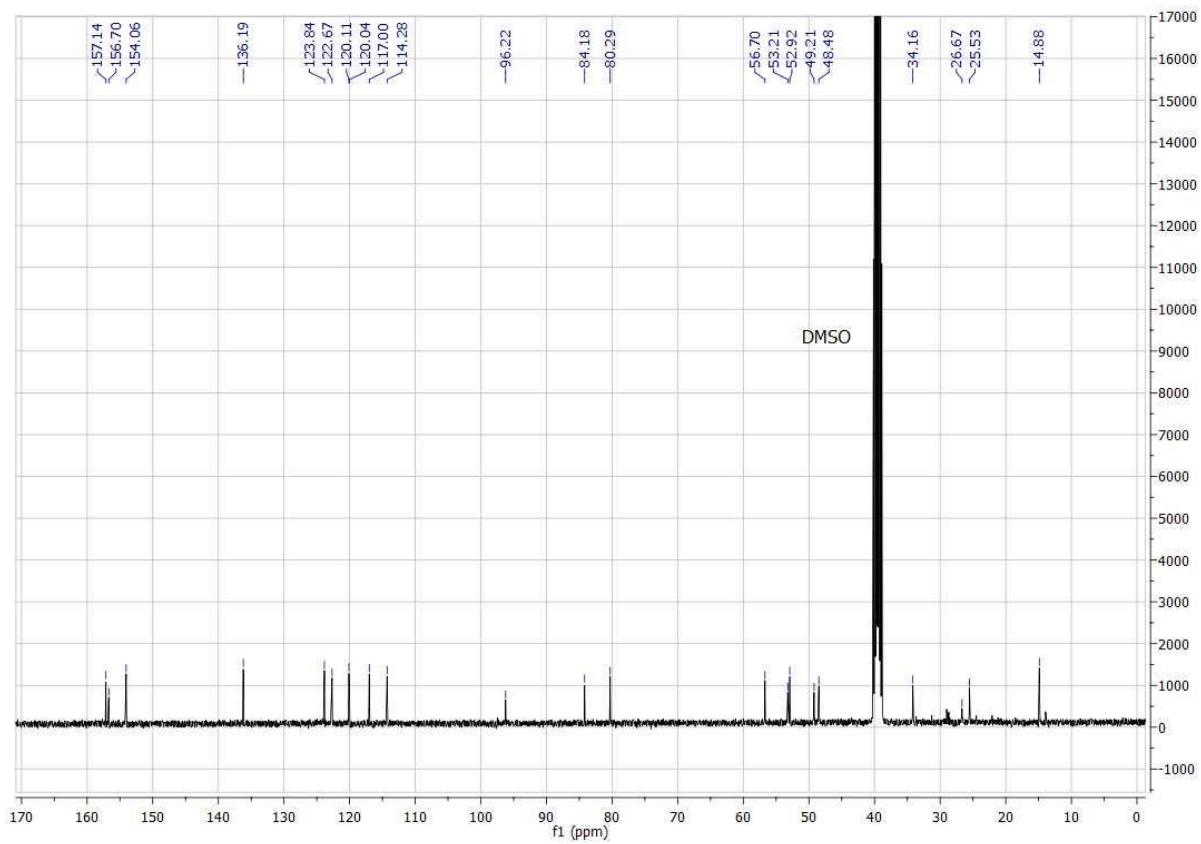
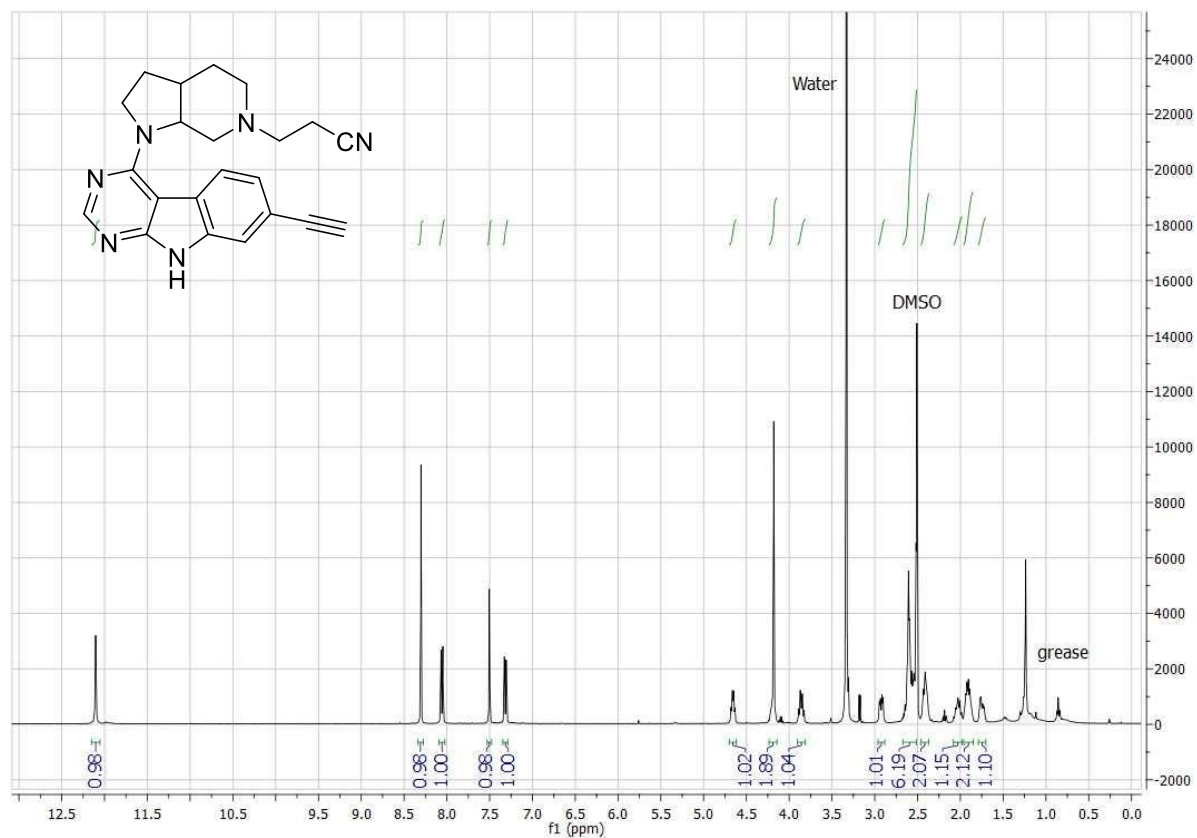
## (S)-5c



(S)-15



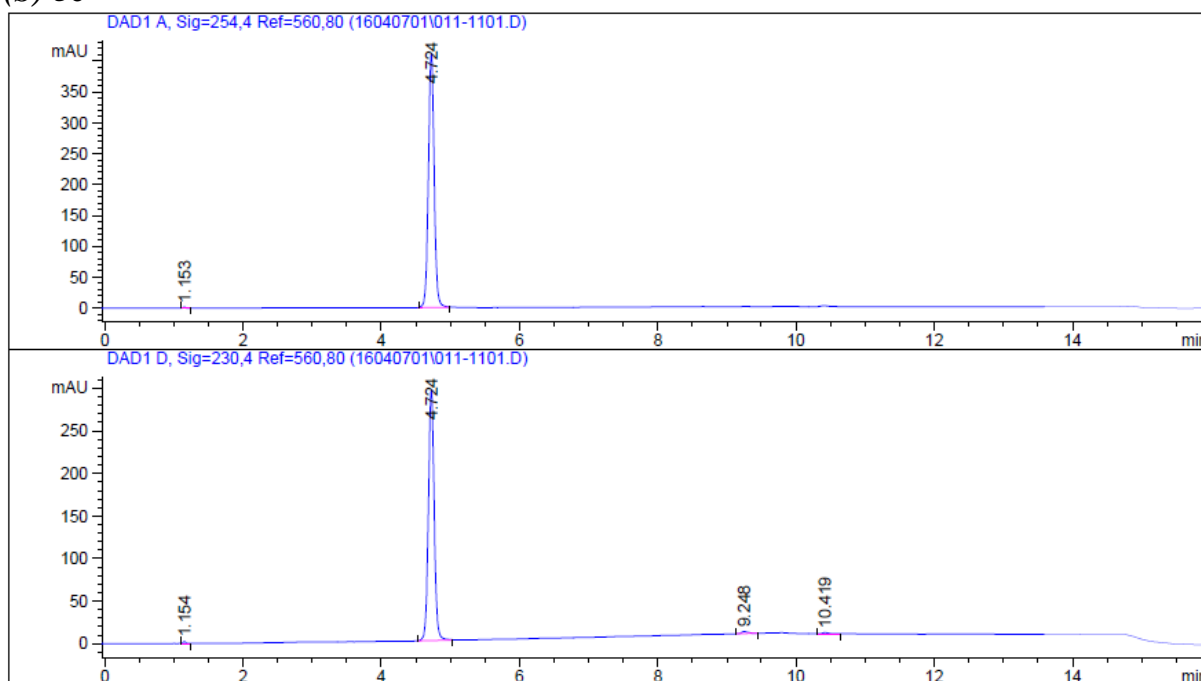






# HPLC chromatograms of (S)-5c, (S)-15, 20 and 22

## (S)-5c



### Area Percent Report

Sorted By : Signal  
Multiplier : 1.0000  
Dilution : 1.0000  
Use Multiplier & Dilution Factor with ISTDs

Signal 1: DAD1 A, Sig=254,4 Ref=560,80

Peak #	RetTime [min]	Type	Width [min]	Area [mAU*s]	Height [mAU]	Area %
1	1.153	BP	0.0389	4.10806	1.78100	0.1717
2	4.724	BB	0.0897	2388.50879	411.59946	99.8283

Totals : 2392.61685 413.38045

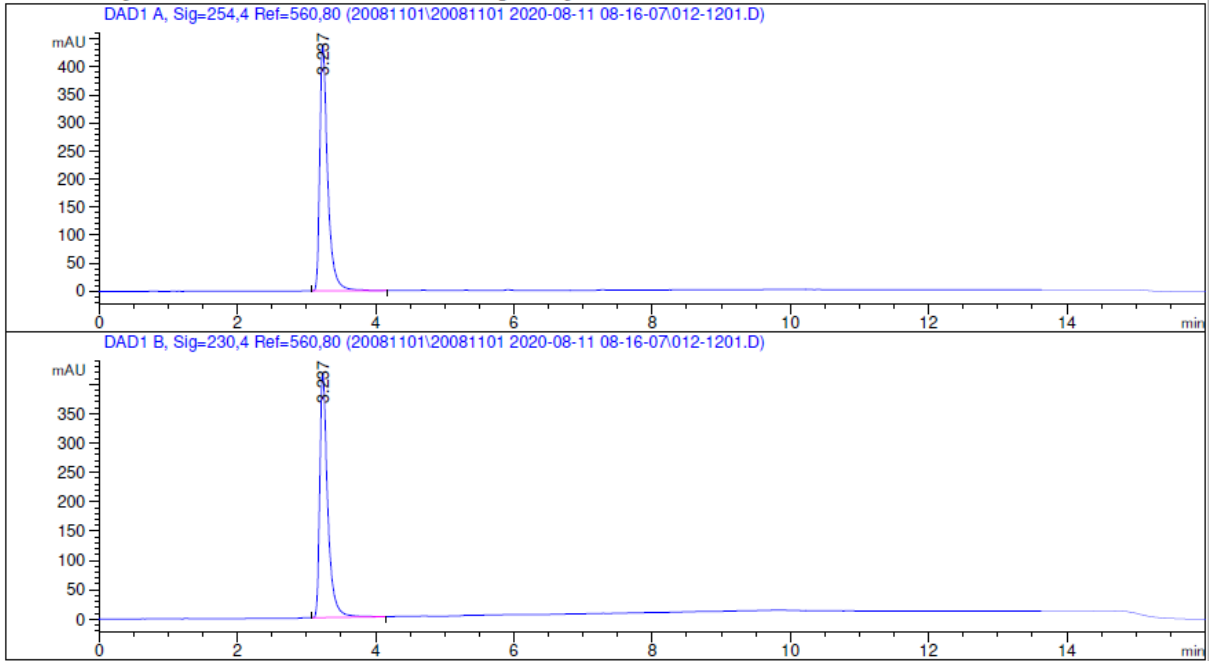
Results obtained with enhanced integrator!

Signal 2: DAD1 D, Sig=230,4 Ref=560,80

Peak #	RetTime [min]	Type	Width [min]	Area [mAU*s]	Height [mAU]	Area %
1	1.154	BP	0.0408	5.73826	2.32211	0.3290
2	4.724	BB	0.0898	1712.81812	294.86554	98.1915
3	9.248	BP	0.0974	16.50928	2.42639	0.9464
4	10.419	PB	0.0965	9.29896	1.41834	0.5331

Totals : 1744.36462 301.03238

(S)-15



=====  
Area Percent Report  
=====

Sorted By : Signal  
Multiplier: : 1.0000  
Dilution: : 1.0000  
Use Multiplier & Dilution Factor with ISTDs

Signal 1: DAD1 A, Sig=254,4 Ref=560,80

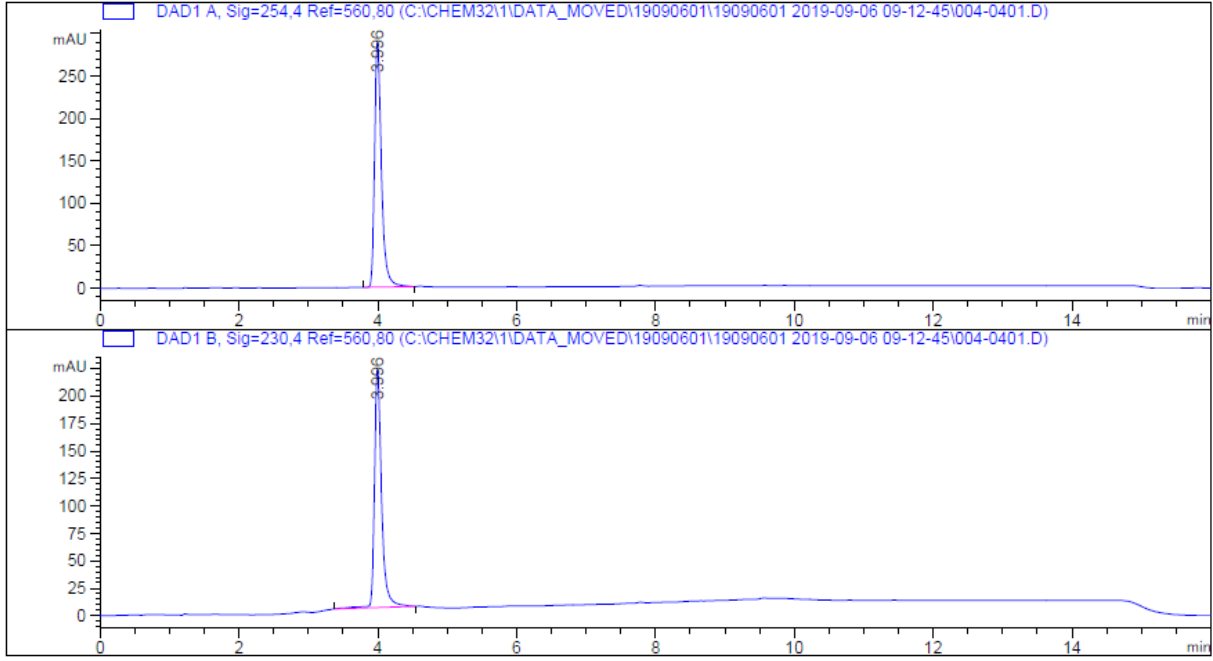
Peak #	RetTime [min]	Type	Width [min]	Area [mAU*s]	Height [mAU]	Area %
1	3.237	BB	0.1168	3502.43384	440.36560	100.0000

Totals : 3502.43384 440.36560

Signal 2: DAD1 B, Sig=230,4 Ref=560,80

Peak #	RetTime [min]	Type	Width [min]	Area [mAU*s]	Height [mAU]	Area %
1	3.237	BB	0.1168	3324.89258	418.22137	100.0000

Totals : 3324.89258 418.22137



=====  
 Area Percent Report  
 =====

Sorted By : Signal  
 Multiplier: : 1.0000  
 Dilution: : 1.0000  
 Use Multiplier & Dilution Factor with ISTDs

Signal 1: DAD1 A, Sig=254,4 Ref=560,80

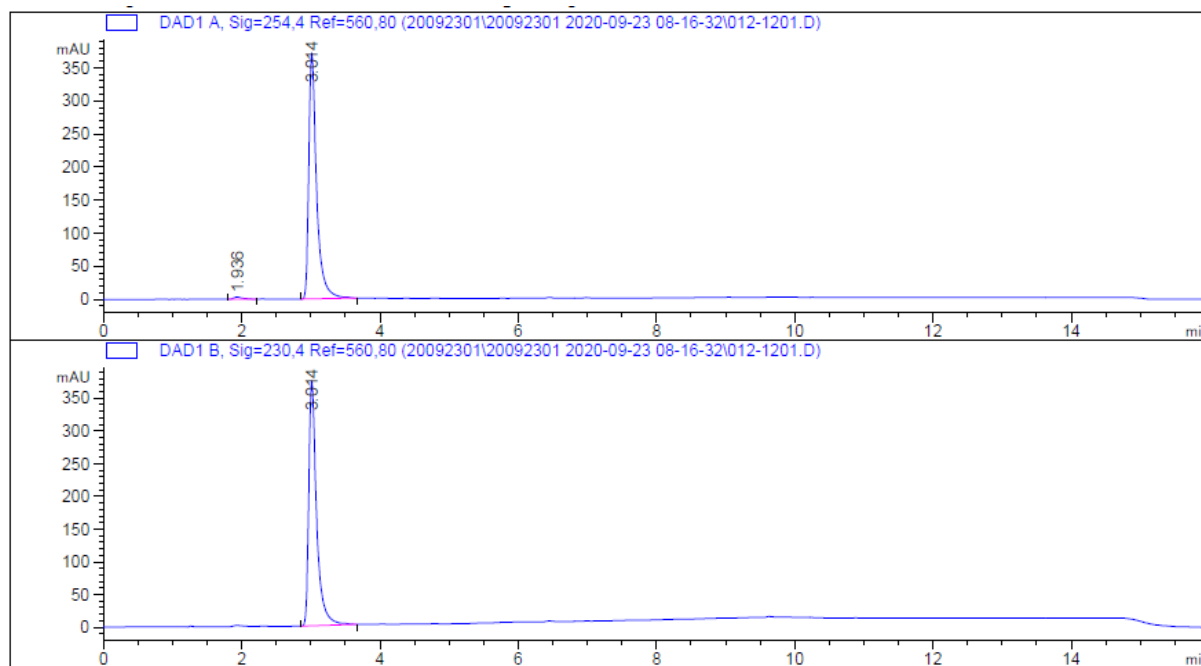
Peak #	RetTime [min]	Type	Width [min]	Area [mAU*s]	Height [mAU]	Area %
1	3.996	BB	0.1040	1979.62488	288.86835	100.0000

Totals : 1979.62488 288.86835

Signal 2: DAD1 B, Sig=230,4 Ref=560,80

Peak #	RetTime [min]	Type	Width [min]	Area [mAU*s]	Height [mAU]	Area %
1	3.996	BB	0.1068	1539.44324	216.92783	100.0000

Totals : 1539.44324 216.92783



=====  
 Area Percent Report  
 =====

Sorted By : Signal  
 Multiplier: : 1.0000  
 Dilution: : 1.0000  
 Use Multiplier & Dilution Factor with ISTDs

Signal 1: DAD1 A, Sig=254,4 Ref=560,80

Peak #	RetTime [min]	Type	Width [min]	Area [mAU*s]	Height [mAU]	Area %
1	1.936	BB	0.1352	28.03933	3.10950	0.9500
2	3.014	BB	0.1158	2923.41162	371.68216	99.0500

Totals : 2951.45095 374.79166

Signal 2: DAD1 B, Sig=230,4 Ref=560,80

Peak #	RetTime [min]	Type	Width [min]	Area [mAU*s]	Height [mAU]	Area %
1	3.014	BB	0.1157	2942.89551	374.27606	100.0000

Totals : 2942.89551 374.27606

## References

1. Bartole, E., Grätz, L., Littmann, T., Wifling, D., Seibel, U., Buschauer, A., Bernhardt, G. UR-DEBa242: a Py-5-labeled fluorescent multipurpose probe for investigations on the histamine H<sub>3</sub> and H<sub>4</sub> receptors. *J. Med. Chem.* **2020**, *63*, 5297-5311.
2. Pruccoli, L., Morroni, F., Sita, G., Hrelia, P., Tarozzi, A. Esculetin as a bifunctional antioxidant prevents and counteracts the oxidative stress and neuronal death induced by amyloid protein in SH-SY5Y cells. *Antioxidants* **2020**, *9*, 551.
3. Tarozzi, A., Morroni, F., Merlicco, A., Hrelia, S., Angeloni, C., Cantelli-Forti, G., Hrelia P. Sulforaphane as an inducer of glutathione prevents oxidative stress-induced cell death in a dopaminergic-like neuroblastoma cell line. *J. Neurochem.* **2009**, *5*, 1161-1171.